Cell Metabolism
Article

MicroRNAs Involved in Molecular Circuitries Relevant for the Duchenne Muscular Dystrophy Pathogenesis Are Controlled by the Dystrophin/nNOS Pathway

Davide Cacchiarelli,[1,4] Julie Martone,[1,4] Erika Girardi,[1] Marcella Cesana,[1] Tania Incitti,[1] Mariangela Morlando,[1] Carmine Nicoletti,[2] Tiziana Santini,[1] Olga Sthandier,[1] Laura Barberi,[2] Alberto Auricchio,[3] Antonio Musarò,[2] and Irene Bozzoni[1,*]

[1]Institute Pasteur Cenci-Bolognetti, Department of Genetics and Molecular Biology and IBPM, "SAPIENZA" University of Rome, P.le A. Moro 5, 00185 Rome, Italy

[2]Department of Histology and Medical Embryology, Interuniversity Institute of Myology, "SAPIENZA" University of Rome, Via A. Scarpa, 14, 00161 Rome, Italy

[3]Telethon Institute of Genetics and Medicine, Via P. Castellino 111, 80131 Napoli, Italy

[4]These authors contributed equally to this work

*Correspondence: irene.bozzoni@uniroma1.it

DOI 10.1016/j.cmet.2010.07.008

SUMMARY

In Duchenne muscular dystrophy (DMD) the absence of dystrophin at the sarcolemma delocalizes and downregulates nitric oxide synthase (nNOS); this alters S-nitrosylation of HDAC2 and its chromatin association. We show that the differential HDAC2 nitrosylation state in Duchenne versus wild-type conditions deregulates the expression of a specific subset of microRNA genes. Several circuitries controlled by the identified microRNAs, such as the one linking miR-1 to the G6PD enzyme and the redox state of cell, or miR-29 to extracellular proteins and the fibrotic process, explain some of the DMD pathogenetic traits. We also show that, at variance with other myomiRs, miR-206 escapes from the dystrophin-nNOS control being produced in activated satellite cells before dystrophin expression; in these cells, it contributes to muscle regeneration through repression of the satellite specific factor, Pax7. We conclude that the pathway activated by dystrophin/nNOS controls several important circuitries increasing the robustness of the muscle differentiation program.

INTRODUCTION

Duchenne muscular dystrophy (DMD) is an X-linked recessive disorder caused by mutations in the dystrophin gene. Its product, dystrophin (427 kDa), links the cytoskeleton to a complex of proteins (dystrophin-associated protein complex, DAPC) on the membrane of muscle fibers (Matsumura et al., 1994). The principal role of DAPC is to connect intracellular actin microfilaments to the extracellular matrix determining a structural stabilization of the sarcolemma (Ervasti and Sonnemann, 2008). The absence of dystrophin in DMD patients leads to a dramatic decrease of the DAPC. As a consequence, muscle fibers become more sensitive to mechanical damage, leading to muscle degeneration, chronic inflammation, susceptibility to oxidative stress, and increased fibrosis, all of which exacerbate the dystrophic phenotype.

Over the past 20 years, the *mdx* mouse, carring a stop codon inside exon 23 of the dystrophin gene, has been widely used as animal model of DMD pathology. Moreover, it provides a convenient system to test possible therapeutic interventions as well as to select molecular markers that could be useful to monitor disease progression and therapeutic outcomes.

It has been shown that most of the mutations in the dystrophin gene can be "cured" at the posttranscriptional level by preventing the inclusion of specific mutant exons in the mature mRNA and recovering a functional open reading frame (Aartsma-Rus et al., 2009). The exon-skipping strategy allows the production of a shorter but still functional dystrophin. This type of proteins are found in Becker muscular dystrophy patients, who generally show milder symptoms than do DMD patients.

Besides its well-defined structural role, the DAPC was shown to influence the intracellular nitric oxide (NO) pathway: the disruption of the association between the sarcolemmal neuronal nitric oxide synthase (nNOS) and DAPC leads to impaired NO production in dystrophic muscles (Brenman et al., 1995). NO has recently emerged as a key player which mediates epigenetic changes through the direct control of histone deacetylases (HDACs). In neurons, a NO-dependent S-nitrosylation of HDAC2 Cys residues (Cys262 and Cys274) induced the activation of genes for neuronal development (Nott et al., 2008). Moreover, in the dystrophin-deficient *mdx* mice, defective for NO pathway, the activity of HDAC2 resulted to be specifically increased (Colussi et al., 2008).

The relevance of NO and HDAC2 activity in the Duchenne pathology is supported by the evidence that rescue of nNOS expression in *mdx* animals ameliorated the dystrophic phenotype (Wehling et al., 2001; Brunelli et al., 2007) and that deacetylase inhibitors conferred a strong morphofunctional benefit to dystrophic muscle fibers (Minetti et al., 2006).

Recent works have shown that among genes which are important for proper muscle development and function, microRNAs (miRNAs) play a crucial role (Naguibneva et al., 2006; Chen et al., 2006). Moreover, altered levels of miRNAs were

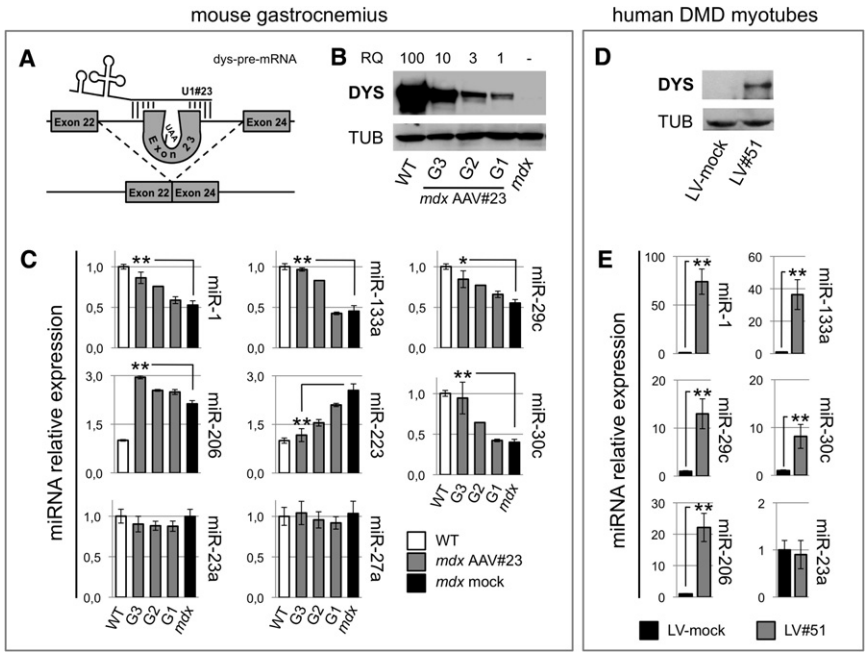

Figure 1. MicroRNA Expression in Duchenne Muscular Dystrophy

(A) Schematic representation of the exon-skipping strategy for *mdx* mutation.

(B) Western blot with anti-dystrophin (DYS) and anti-tubulin (TUB) antibodies performed on protein extracts from the gastrocnemius of WT, *mdx*, and AAV#23-treated *mdx* (G1, G2, and G3) animals, sacrificed 4 weeks after systemic virus injection. Dystrophin relative quantifications are shown on the top of each lane.

(C) Histograms show miRNA relative expression in WT, G1-G3, and *mdx* mice, measured by qRT-PCR. miR-23a and miR-27a were used as controls. Expression levels were normalized to snoRNA55 and shown with respect to WT set to a value of 1.

(D) Western blot with DYS and TUB antibodies on protein extracts from human DMD myoblasts infected with LV#51 (LV#51) or control (LV-mock) lentiviruses and differentiated for 7 days.

(E) Histograms show miRNA relative expression in LV-mock and LV#51-treated DMD cells measured by qRT-PCR. U6 snRNA was used as endogenous control. Relative expressions are shown with respect to LV-mock DMD cells, set to a value of 1. *$p < 0.05$, **$p < 0.01$.

found in several muscular disorders such as myocardial infarction (van Rooij et al., 2008a), DMD, and other myopathies (Eisenberg et al., 2007; Greco et al., 2009).

In this work we took advantage of the exon-skipping strategy to study whether the recovery of the dystrophin/nNOS pathway correlated with the expression of miRNAs relevant for the DMD physiopathology. We described that the activation of the NO signaling modulates HDAC2 association with a specific subset of miRNA genes and alteration of their expression correlates with several pathogenetic traits of Duchenne disease.

RESULTS

The Expression Levels of Specific miRNAs Correlate with the Amount of Dystrophin

Six-week-old *mdx* animals were tail vein injected with a recombinant adeno-associated viral vector carrying a U1-chimeric antisense construct (AAV#23) previously reported to induce the skipping of the mutated exon 23 and to restore dystrophin synthesis (Figure 1A and Denti et al., 2006). After 1 month, *mdx* and AAV#23-treated *mdx* siblings were sacrificed in parallel with wild-type (WT) isogenic/aged matched animals. Different muscular districts (gastrocnemius, diaphragm, triceps, and quadriceps) were dissected and tissue collected for protein, RNA, and chromatin analyses. Western blot revealed that through the exon-skipping treatment, rescue of dystrophin was obtained in all districts (data not shown), confirming the previously described body-wide activity of the AAV#23 virus. Due to individual variability in the systemic delivery of AAV, we were able to classify injected animals in three different groups (G1, G2, and G3), which displayed $\leq$1%, 1%–5%, and 5%–10% of dystrophin rescue, respectively. A representative sample of each group is shown in Figure 1B.

Real-time based low density arrays revealed that the expression of a subset of miRNAs deregulated in *mdx* animals was restored toward WT levels in AAV#23-treated mice (underlined in Figure S1A and Table S1, available online).

Among the miRNAs analyzed by array, we validated by qRT-PCR those showing the most prominent variations. Since homologous members of miR-29, miR-30, and miR-133 families were equally deregulated, we focused our analysis on one member per family. The muscle-specific (myomiR) miR-1 and miR-133 (van Rooij et al., 2008b) and the ubiquitous miR-29c and miR-30c, downregulated in *mdx*, recovered toward WT levels in exon-skipping-treated animals (Figure 1C). A direct correlation between miRNA levels and dystrophin rescue was observed: G1 animals showed a very limited miRNA recovery, while G3 displayed levels close to WT ones (Figure 1C).

At variance with the other myomiRs, miR-206 was highly expressed in *mdx* as well as in AAV#23-treated animals. Interestingly, even if miR-206 was described on the same cluster with miR-133b, suggesting that they may be transcribed together, in *mdx* muscles miR-206 increases while miR-133b decreases. Chromatin immunoprecipitation (ChIP) analysis for RNA polymerase II and histone-H3-lysine-9 acetylation (AcH3K9) (Figure S1D) and pri-miRNA quantifications (Figure S1E) in WT versus *mdx* muscles indicated a higher transcriptional activity on miR-206 coding region with respect to miR-133b, suggesting that the two miRNAs are under an independent control.

The inflammatory miR-223 (Fazi et al., 2005), specific of granulocytic lineage, was found to be very abundant in *mdx* muscles and proportionally reduced in the three groups of treated animals; its decrease in AAV#23-*mdx* is consistent with the observed amelioration of the inflammatory state of the muscle due to dystrophin rescue (Denti et al., 2008; Aartsma-Rus et al., 2009). Finally, the expression levels of the ubiquitous miR-23a and miR-27a were unchanged in WT and *mdx*, as well as in treated animals.

The relative changes in the expression patterns of miR-1, miR-29, miR-206, and miR-223 observed in the gastrocnemius were confirmed in other muscle districts (data not shown),

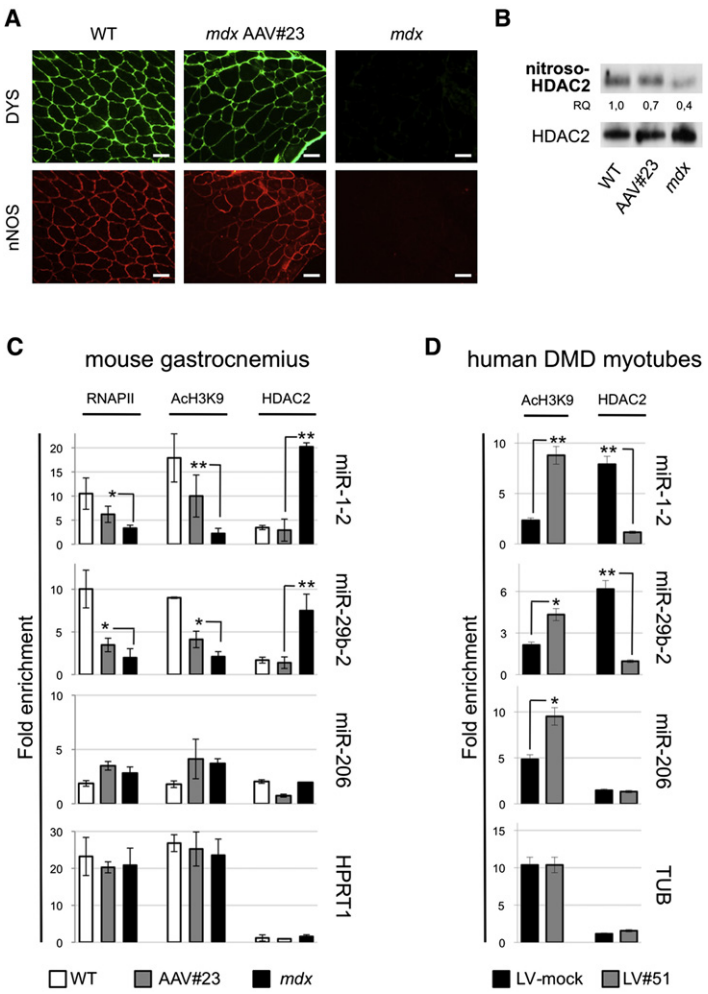

Figure 2. Dystrophin/nNOS Relocalization Modulates HDAC2 Occupancy on miRNA Loci

(A) Gastrocnemius from WT, AAV#23-treated *mdx*, and control *mdx* mice were analyzed by immunofluorescence with DYS and nNOS antibodies. Original magnification, ×20. Scale bar, 100 μm.

(B) Protein extracts from the gastrocnemius of WT, AAV#23-treated *mdx* (AAV#23) and control *mdx*, were immunoprecipitated with antibody against nitrosylated-Cys residues and assayed for HDAC2 by western blot (nitroso-HDAC2). Below each lane the relative quantities (RQ) with respect to WT are indicated. Values are normalized for the amount of total HDAC2 (HDAC2) and represent the average of three independent experiments.

(C and D) ChIP analyses performed on miR-1-2/133a, miR-29b-2/29c, and miR-206 promoters (see schematic representation in Figure S2B). (C) Histograms show RNA polymerase II (RNAPII), AcH3K9, and HDAC2 enrichments in WT, AAV#23, and *mdx* gastrocnemius. (D) Histograms show AcH3K9 and HDAC2 enrichments in control (LV-mock) and antisense-treated (LV#51) DMD myoblasts. HPRT1 and tubulin (TUB) promoter regions were used as unrelated transcriptional units, while 5.8S rRNA and tRNA genes were used as internal negative controls (see representative gels in Figures S2C and S2D). Results are expressed as fold enrichment of DNA-immunoprecipitated samples relative to INPUT chromatin. *$p < 0.05$, **$p < 0.01$.

demonstrating that the miRNA expression profile correlated with dystrophin rescue in a body-wide manner. Moreover, injections of *mdx* mice with an AAV empty vector indicated that virus adminstration per se did not affect miRNA expression (Figure S1B).

The observation that the expression of a specific subset of miRNAs varies in response to dystrophin prompted the analysis in a human Duchenne model system. Differentiating DMD myoblasts, carrying a deletion of exons 48–50, were treated with a lentiviral construct expressing an antisense RNA able to induce exon 51 skipping (LV#51) or with an empty vector (LV-mock). This treatment was previously shown to produce an in-frame mRNA and to rescue dystrophin synthesis (De Angelis et al., 2002; Incitti et al., 2010). According to the *mdx* model, when dystrophin synthesis was restored (Figure 1D), the levels of miR-1, miR-133a, miR-29c, miR-30c, and miR-206 increased, while miR-23a expression did not change (Figure 1E).

HDAC2 Controls the Expression of Specific miRNA Genes

Immunofluorescence analyses (Figure 2A) were performed with anti-dystrophin and anti-nNOS antibodies on sections from the gastrocnemius of WT, *mdx*, and G3 *mdx* (AAV#23). Upon exon-skipping treatment, dystrophin synthesis and correct localization to the periphery of the fibers were obtained (DYS); moreover, the restoration of dystrophin paralleled the proper colocalization of nNOS to the DAPC (nNOS). The morphological amelioration of the muscles transduced with AAV#23 was also observed by hematoxylin and eosin staining (Figure S2A).

One interesting target of nNOS was shown to be the HDAC2 chromatin-remodeling enzyme (Nott et al., 2008; Colussi et al., 2008). Therefore, we tested whether HDAC2 was differentially nitrosylated in WT, *mdx*, and AAV#23-treated *mdx* animals. Protein extracts were immunoprecipitated with anti-nitrosocysteine antibody and subsequently analyzed by western blot for HDAC2. The lowest level of nitrosylated HDAC2 was found in *mdx* mice; progressive increase of HDAC2 nitrosylation was detected in AAV#23 and WT muscles (Figure 2B). These data provided a correlation between nitrosylation state of HDAC2 and dystrophin levels.

Since the nitrosylation state of HDAC2 was found to affect its association to the chromatin (Nott et al., 2008), we tested whether altered levels of miRNAs in *mdx* were due to HDAC2 recruitment to their promoters. We selected the miR-1 and miR-29 promoters, since they have been previously characterized (see Figure S2B and Rao et al., 2006; Liu et al., 2007; Wang et al., 2008). ChIP analysis with antibodies against RNA polymerase II (Lee et al., 2004) and AcH3K9 showed low binding levels in *mdx* and progressive increase in G3 (AAV#23) and WT animals (Figure 2C). These data indicated a good correlation between the transcriptional state of these loci and the expression levels of the corresponding miRNAs (Figure 1C), confirming that variations in miRNA expression depended on transcriptional control. ChIP with anti-HDAC2 antibody revealed its specific binding with miR-1 and miR-29 promoters only in *mdx* mice (Figure 2C) where these miRNAs are downregulated. No reactivity was observed with either HDAC1 or HDAC4. On the

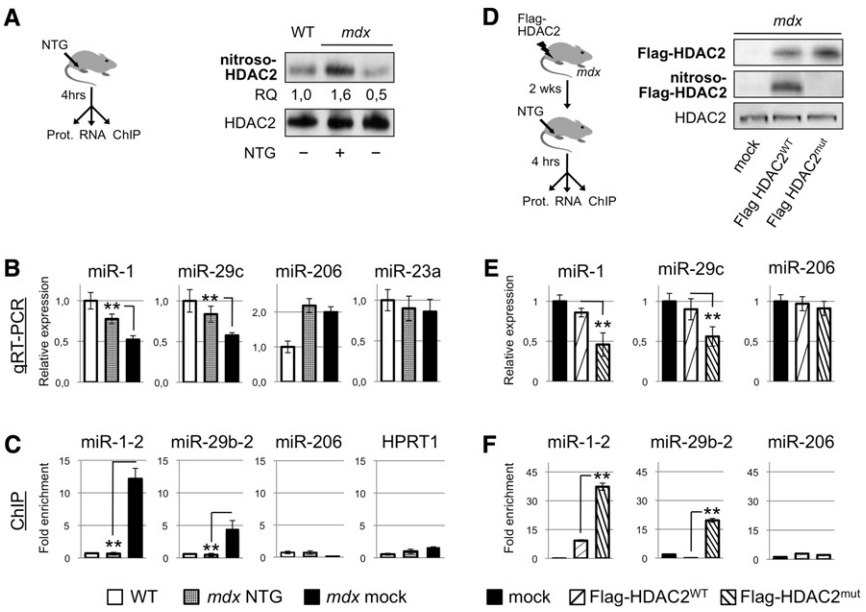

Figure 3. NO Signaling Controls miRNA Expression through HDAC2 Nitrosylation

(A–C) mice were injected with nitroglycerin (NTG) into the right gastrocnemius and with physiological solution into the left one. After 4 hr, protein, RNA, and chromatin samples were collected. (A, right panel) Proteins were immunoprecipitated with antibody against nitrosylated-Cys residues and assayed for HDAC2 by western blot (nitroso-HDAC2). Below each lane the relative quantities (RQ) with respect to WT are indicated; values are normalized for the amount of total HDAC2 (HDAC2) and represent the average of three independent experiments. (B) Histograms show miRNA relative expression measured by qRT-PCR in NTG-treated (*mdx* NTG) or mock-injected (*mdx* mock) *mdx* muscles with respect to WT one set to a value of 1. Relative expressions were normalized to snoRNA55. (C) ChIP analyses for HDAC2 on miR-1-2/133a, miR-29b-2/29c, and miR-206 promoters in WT, *mdx* NTG, and *mdx* mock muscles. HPRT1 promoter region was used as unrelated transcriptional unit while 5.8S rDNA was used as an internal negative control. Results are expressed as fold enrichment of DNA immunoprecipitated samples relative to INPUT chromatin.

(D–F) *mdx* mice were electroporated into the right tibialis with expression cassettes encoding for a WT flagged HDAC2 protein (Flag-HDAC2^{WT}) or for a derivative mutated at Cys262 and Cys274 (Flag-HDAC2^{mut}). After 2 weeks mice were injected with NTG into the right tibialis and with physiological solution into the left one (mock). After 4 hr protein, RNA and chromatin samples were collected. (D, right panel) Expression levels of flagged HDAC2 were assayed by western blot with anti-Flag antibody (Flag-HDAC2). Nitrosylation state was revealed by immunoprecipitation with anti-Flag antibody followed by western blot using an antibody against nitrosylated-Cys residues (nitroso-Flag-HDAC2). (E) Histograms show miRNA relative expression measured by qRT-PCR in mock-, Flag-HDAC2^{WT}-, and Flag-HDAC2^{mut}-treated muscles. Expression levels were normalized to snoRNA55 and shown with respect to mock set to a value of 1. (F) ChIP analyses were performed with anti-Flag antibody on miR-1-2/133a, miR-29b-2/29c, and miR-206 promoters in mock, Flag-HDAC2^{WT}, and Flag-HDAC2^{mut} treated muscles. Results are expressed as fold enrichment of DNA immunoprecipitated samples relative to INPUT chromatin. $^{**}p < 0.01$.

contrary, the miR-206 promoter (characterized by M.C. and D.C., unpublished data) did not reveal any HDAC2 interaction.

ChIP analyses were carried out also in human differentiating DMD myoblasts infected with the lentiviral construct expressing an antisense RNA (LV#51) able to rescue dytrophin synthesis. The results indicated that also in this system the upregulation of miR-1 and miR-29 correlated with release of HDAC2 from their promoters and changes in histone acetylation state (Figure 2D). Also in DMD cells no HDAC2 interaction was detected on miR-206 promoter. These data indicate that both in murine and human dystrophic cells the absence of dystrophin correlates with HDAC2 binding to a specific subset of miRNAs, while upon dystrophin rescue HDAC2 is released from these promoters.

Nitric Oxide Signaling Controls miRNA Expression through HDAC2 Modification

Local injection of the NO-donor nitroglycerin (NTG) was utilized as a way of inducing NO response to specific body districts. Leg muscles of *mdx* animals were injected with NTG, or physiological solution as control, and dissected after 4 hr. Immunoprecipitation with antibody against nitrosylated cysteine residues and subsequent HDAC2 western blot analysis indicated that NTG treatment rescues the nitrosylated levels of HDAC2 to WT values (Figure 3A). qRT-PCR and ChIP analysis were performed to measure miRNA levels and HDAC2 association to the corresponding promoters. The data show that NTG treatment in *mdx* mice (1) increases miR-1 and miR-29 expression (Figure 3B), (2) induces HDAC2 release from the promoters of these miRNAs (Figure 3C), and (3) has no effect on miR-206.

To further prove the role of HDAC2 nitrosylation on miRNA control, *mdx* muscles were electroporated with expression cassettes encoding for a WT flagged-HDAC2 protein or for a derivative mutated at the two cysteines (Cys 262 and Cys 274) known to be the target of nitrosylation (Nott et al., 2008). Two weeks after treatment, NTG was locally injected and samples extracted for protein, RNA, and chromatin analyses. Figure 3D shows that both exogenous proteins are expressed in the electroporated tissues (Flag-HDAC2) and only the WT form can be nitrosylated (nitroso Flag-HDAC2). ChIP experiments with anti-Flag antibodies showed that, upon NTG treatment, WT Flag-HDAC2 was released from miR-1 and miR-29 promoters (Figure 3F), paralleling the increase of the corresponding miRNAs (Figure 3E); on the contrary, the mutant Flag-HDAC2 protein remained bound to the promoters producing their down-regulation (Figures 3E and 3F). No differences were observed on the HDAC2-independent miR-206 promoter.

Altogether, these results demonstrate that NO induces HDAC2 nitrosylation, thus regulating its binding on specific miRNA promoters.

miR-206 Activates Satellite Cell Differentiation through Pax7 Repression

The differential behavior of miR-1 and miR-206 in WT versus *mdx* prompted us to analyze in more detail their pattern of expression.

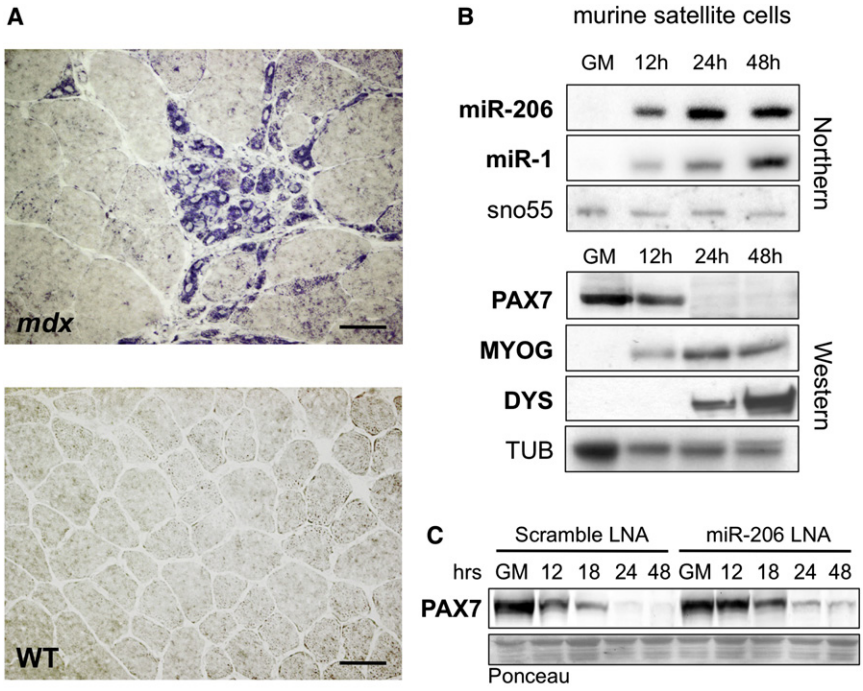

Figure 4. miR-206 Expression and Function

(A) A miR-206 DIG-labeled probe was hybridized on *mdx* and WT gastrocnemius sections. Original magnification, ×40. Scale bar, 50 μm.

(B) RNA and protein samples were extracted from proliferating satellite cells (GM, growth medium) and after shift to differentiation medium (DM) for the indicated hours. (Upper panels) Northern blots for miR-206, miR-1, and snoRNA55; (lower panels) western blots for PAX7, myogenin (MYOG), dystrophin (DYS), and tubulin (TUB).

(C) Western blot for PAX7 on protein extracts of murine satellite cells transfected with anti-miR-206 or scramble LNA oligos in GM and switched to DM for the indicated hours. Ponceau staining was used as loading control.

(D) miR-1, miR-206, and U2 snRNA expression analyzed by northern blot in C2 myoblasts maintained in GM or in DM for 5 days.

(E) ChIP analysis on miR-1-2/133a and miR-206 promoters with antibodies against AcH3K9, HDAC2, and HDAC1 on chromatin from C2 cells in GM and DM (see representative gels in Figure S2E). 5.8S rDNA was used as internal negative control. Results are expressed as fold enrichment of DNA immunoprecipitated samples relative to INPUT chromatin. **$p < 0.01$.

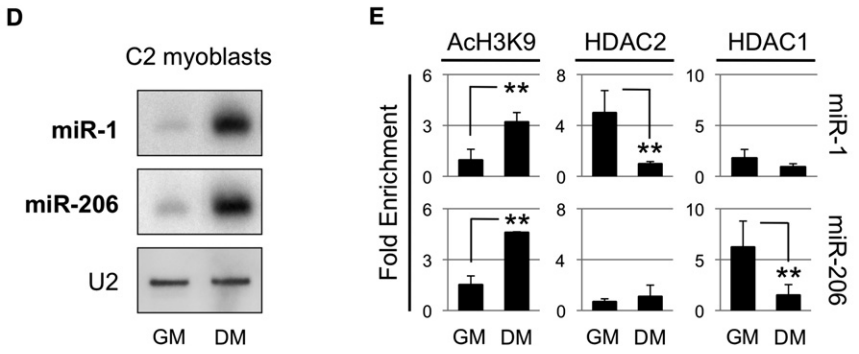

These miRNAs, while sharing the same seed, differs only for four nucleotides in the 3′ portion. In situ hybridization analysis was performed on *mdx* and WT gastrocnemius by using DIG-labeled probes. Signals for miR-206 were restricted to *mdx* and only in immature regenerating fibers with centralized nuclei (Figure 4A), whereas the miR-1 probe showed intense accumulation in mature differentiated fibers in both WT and *mdx* fibers (Figure S3A). Intact multinucleated fibers and small mononucleated cells, such as inflammatory cells, fibroblasts, and proliferating satellite cells, lacked the miR-206 signals (note the absence of signals in interstitial spaces where this type of cell is visualized by DAPI staining in Figure S3A). Therefore, increased expression of miR-206 in *mdx* muscles is due to differentiating satellite cells (Yuasa et al., 2008).

Next, we isolated mouse satellite cells from muscle biopses and differentiated them in vitro (Rando and Blau, 1994). miR-206 expression was activated at 12 hr, and its accumulation proceeded during differentiation (Figure 4B, upper panel). Notably, the satellite-specifying factor Pax7 (Relaix et al., 2006), abundant in growth conditions, started to decrease at 12 hr and completely disappeared at 24 hr, therefore showing an inverse correlation with miR-206 levels (Figure 4B, lower panel). Moreover, transfection of in vitro-cultured satellite cells with anti-miR-206 LNA oligonucleotides indicated that in the absence of miR-206, Pax7 repression was unaffected at 12 hr and remained detectable up to 48 hr (Figure 4C and Figure S3B). The link between Pax7 decrease, miR-206 induction, and the presence of miR-206 putative target sites in the 3′UTR of Pax7 mRNA led us to study whether a regulatory interaction exists. Luciferase assays on reporter constructs allowed us to validate the Pax7 3′UTR as a specific target of miR-206 (Figures S3C and S3D). These experiments indicated that Pax7 can be repressed also by miR-1; however, as shown in the Northern blot of Figure 4B, in cultured satellite cells miR-1 is almost undetectable at 12 hr when downregulation of Pax7 starts, allowing us to conclude that mainly miR-206 is expressed at a time compatible with Pax7 repression. Therefore, these data demonstrate that miR-206 plays a specific role in early events of regeneration by repressing the activity of Pax7, thus allowing the progression of the differentiation program.

ChIP analysis for HDACs binding on the miR-1 and miR-206 loci in conditions of miRNA repression (GM, growth medium) versus miRNA activation (DM, differentiation medium) in C2 myoblasts indicated that, differently from miR-1, miR-206 is specifically repressed by HDAC1 (Figures 4D and 4E). The restricted expression of miR-206 in early phases of

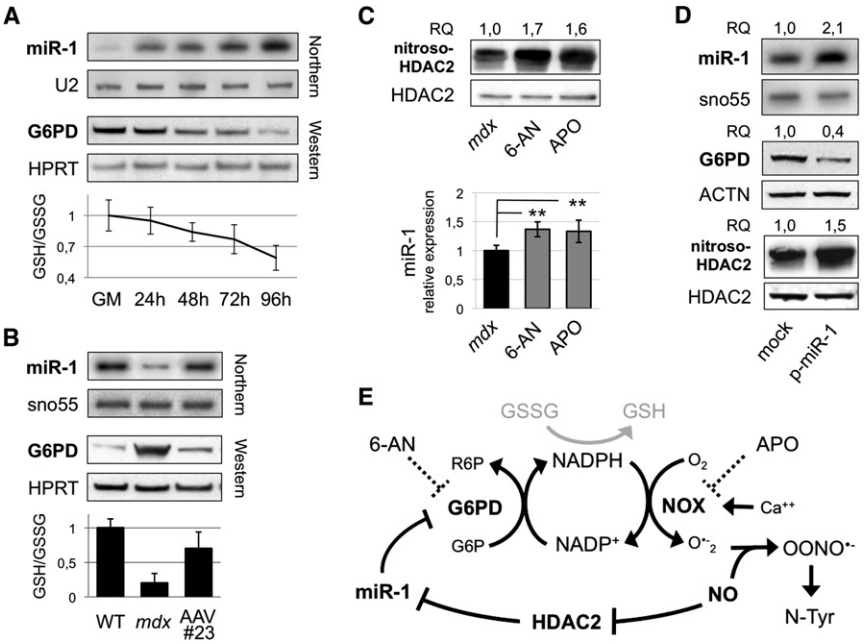

Figure 5. miR-1 Controls G6PD Expression

(A) Total RNA and protein extracts, from C2 proliferating myoblasts (GM, growth medium) and after shift to differentiation medium (DM) for the indicated hours. (Upper panels) Northern blot (miR-1 and U2 snRNA), (middle panels) western blot (G6PD and HPRT1), (lower panel) GSH and GSSG ratio obtained by enzymatic assay titration.

(B) Total RNA and protein extracts from WT, *mdx*, and AAV#23-treated *mdx*. (Upper panels) Northern blot (miR-1 and snoRNA55), (middle panels) western blot (G6PD and HPRT1), (lower panel) GSH and GSSG ratio obtained by enzymatic assay titration.

(C) (Upper panel) Protein extracts, from the gastrocnemius of control *mdx* (*mdx*) and *mdx* treated with G6PD (6-AN) or NOX (APO) inhibitors, were immunoprecipitated with antibodies against nitrosylated-Cys residues and analyzed for HDAC2 content by western blot (nitroso-HDAC2). On the top of each lane the relative quantities (RQ) of nitroso-HDAC2 normalized for the amount of total cellular HDAC2, with *mdx* set to a value of 1, are indicated. Values are the average of three independent experiments. (Lower panel) qRT-PCR for miR-1 on *mdx*, 6-AN, and APO *mdx*-treated mice. Relative expressions were normalized to snoRNA55 and shown with respect to *mdx* set to a value of 1.

(D) *mdx* animals were electroporated with a miR-1 expression construct (p-miR-1) in the right gastrocnemius or with an empty vector (*mock*) in the controlateral muscle and sacrificed after 25 days. miR-1, G6PD, and nitroso-HDAC2 levels were measured. Relative quantities (RQ), shown with respect to *mdx* set to a value of 1, are indicated. The values are the average of three independent experiments. snoRNA55, ACTN, and HDAC2 were used for normalization.

(E) Pathway connecting G6PD, NOX, NO, HDAC2, and miR-1. $^{**}p < 0.01$.

differentiation, before dystrophin synthesis starts, well correlates with its expression being unaffected by the Dys/nNOS/HDAC2 pathway.

miR-1 Controls G6PD, a Relevant Enzyme in the Response to Oxidative Stress

In silico analysis, performed by comparing mRNA expression profiles in WT versus *mdx* animals (Tseng et al., 2002), identified a large number of predicted targets of those miRNAs showing the highest variations in our analysis. For the downregulated miR-1, miR-29, and miR-30, several upregulated targets relevant in muscle physiology were found, such as those involved in energetic metabolism, cytoskeleton remodeling, extracellular matrix, and transcriptional regulation in muscle (Figure S4).

One important issue in dystrophic muscles is their susceptibility and response to oxidative stress suggested to be involved in disease progression (Rando et al., 1998). Glucose-6-phosphate dehydrogenase (G6PD) mRNA, deregulated in *mdx* muscles, contains in its 3′UTR three putative binding sites for the miR-1 family (see Figure S5A).

G6PD is a cytosolic enzyme in the pentose phosphate pathway that supplies reducing energy to cells by maintaining the level of NADPH, which in turn ensures high ratio between reduced and oxidized glutathione (GSH/GSSG), GSH being the major antioxidant molecule that protects cells against oxidative damage.

Luciferase reporter assays validated G6PD mRNA as a target of the miR-1 family. Figure S5E shows that miR-1 and miR-206 are able to repress luciferase activity only in the presence of a WT G6PD-3′UTR and that this repression is alleviated by anti-miR-1 and anti-miR-206 LNA oligonucleotides.

Several data indicated an inverse correlation between G6PD and miR-1 expression: in vitro differentiation of C2 myoblasts showed that the increase in miR-1 levels (Figure 5A, upper panel) correlated with decrease of G6PD protein (Figure 5A, middle panel), mRNA levels (Figure S5B), and GSH/GSSG ratio (Figure 5A, lower panel). Figure 5B shows that in *mdx* mice, where miR-1 is downregulated, G6PD was detected at higher levels than in WT muscles, whereas in AAV#23-treated *mdx*, in which miR-1 resumes, the amount of G6PD was reduced. Notably, in *mdx* mice, increase in G6PD levels was accompanied by a decrease in GSH/GSSG ratio (Figure 5B, lower panel). This apparent contradiction can instead be explained considering that in *mdx* muscles, most of the NADPH is utilized in the O_2 to $O^{\cdot-}_2$ conversion mediated by the Ca^{2+}-dependent activation of NADPH oxidase (NOX; Shkryl et al., 2009). Detoxification of the superoxide radical could further reduce NO levels already low in *mdx*. Therefore, we asked whether interfering with this pathway could affect the nitrosylation state of HDAC2. When G6PD was inactivated through administration of 6-aminonicotinamide (6-AN; Walker et al., 1999), HDAC2 nitrosylation increased as well as the levels of miR-1 (Figure 5C). In line with this, NOX inhibition with apocynin (APO; Gupte et al., 2006) also increased HDAC2 nitrosylation and miR-1 levels (Figure 5C).

Finally, G6PD downregulation through overexpression of miR-1 (p-miR-1) in *mdx* muscles increased HDAC2 nitrosylation

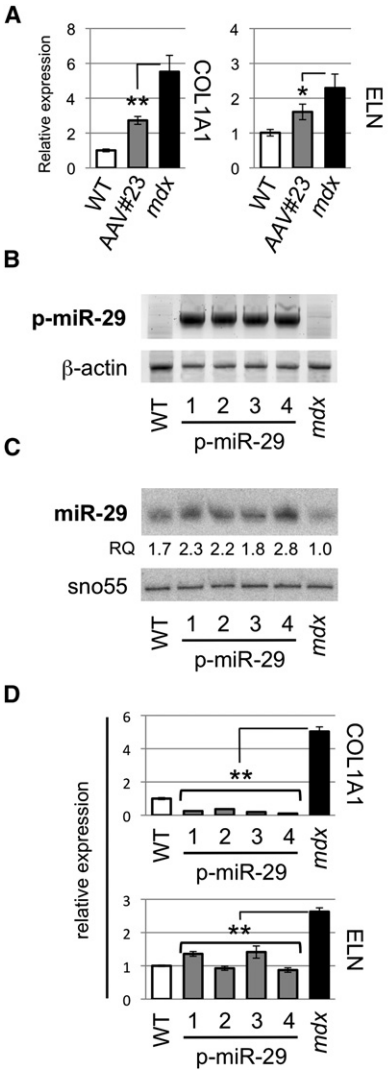

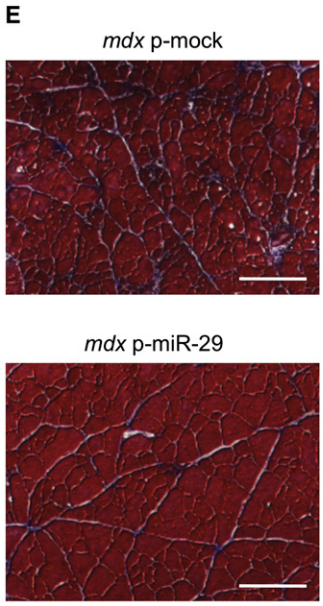

Figure 6. miR-29 Controls Fibrosis in *mdx*

(A) qRT-PCR for collagen (COL1A1) and elastin (ELN) mRNAs performed on total RNA from the gastrocnemius of WT, AAV#23-treated *mdx*, and *mdx* mice. Relative expressions were normalized to HPRT1 and shown with respect to WT set to a value of 1. In (B)–(E) the gastrocnemius of *mdx* animals was electroporated with a miR-29a/b expression construct (p-miR-29) and sacrificed after 25 days in parallel with WT and a control *mdx* electroporated with an empty plasmid (*mdx*).

(B) PCR analysis on DNA from WT, *mdx*, and p-miR-29 electroporated (1–4) *mdx*. Primers specific for the p-miR-29 construct and for the β-actin gene were utilized.

(C) Northern blot for miR-29 and control snoRNA55. Relative quantities (RQ) of miR-29, relative to *mdx* set to a value of 1, are indicated below each lane.

(D) qRT-PCR on COL1A1 and ELN mRNAs. Relative expressions are normalized to HPRT1 mRNA. Values are shown with respect to WT set to a value of 1.

(E) Masson's trichrome staining indicates collagen deposition (blue stain) on p-mock and p-miR-29 electroporated *mdx*. Original magnification, ×10. Scale bar, 100 μm. *$p < 0.05$, **$p < 0.01$.

with respect to control (Figure 5D). The link between G6PD, NO, HDAC2, and miR-1 in *mdx* is shown in Figure 5E; namely, in conditions of increased levels of G6PD more $O^{\circ-}_2$ radicals, deriving from the activity of NOX, are converted to $ONOO^{\circ-}$. This reduced both NO levels and HDAC2 nitrosylation. Altogether, these data demonstrate that all these components are on the same pathway and that a feed-forward control between G6PD and miR-1 through the S-nitrosylation of HDAC2 exists.

miR-29 Controls Fibrosis in *mdx* Muscles

mdx animals undergo extensive fibrotic degeneration (Haslett et al., 2002). Crucial factors involved in this event are collagens and elastin, structural components of the extracellular matrix, whose mRNAs have been recently shown to be targeted by miR-29 family in myocardial infarction (van Rooij et al., 2008a). qRT-PCR revealed that in *mdx*, where miR-29 is poorly expressed, the mRNAs for collagen (COL1A1) and elastin (ELN) were upregulated. Their amount was instead reduced at levels similar to WT in AAV#23-treated animals, where miR-29 levels were resumed (Figure 6A). In order to test whether miR-29 alone is able to regulate collagen and elastin mRNAs in the Duchenne fibrotic process, we electroporated in the gastrocnemius of *mdx* animals a plasmid DNA containing an expression cassette driving the transcription of the miR-29a/b cluster (p-miR-29). Control *mdx* mice were electroporated with an empty plasmid. Twenty-five days after treatment, muscles were dissected, and the presence of p-miR-29 DNA was verified by PCR (Figure 6B). Northern blot indicated that a 2- to 3-fold overexpression of miR-29 was specifically obtained (Figure 6C) and that this paralleled a relevant decrease of collagen and elastin mRNAs (Figure 6D). Trichromic staining on *mdx* mice electroporated with p-miR-29 indicated a strong decrease in collagen deposition (blue stain) if compared to mock-electroporated muscles (Figure 6E). These data point to miR-29 as a crucial player in the control of the extracellular matrix modifications in *mdx* mice.

DISCUSSION

In DMD, muscle fiber breakage and degeneration, due to the absence of dystrophin, are accompanied by a complex series of events including activation of satellite cells, inflammatory infiltration, intense fibrosis, and oxidative stress. These pathogenetic features are ameliorated in *mdx* mice, in which dystrophin is rescued through different therapeutic strategies (Aartsma-Rus et al., 2009). Surprisingly, the beneficial effects observed on muscle function and morphology could be obtained also with low levels of protein (Denti et al., 2008; Ghahramani Seno et al., 2008), suggesting that partial protein relocalization to the membrane could be only part of the story. Dystrophin has been suggested to affect gene expression through activation of the NO pathway and HDAC2 regulation (Colussi et al., 2009); however, no specific genes and regulatory circuitries

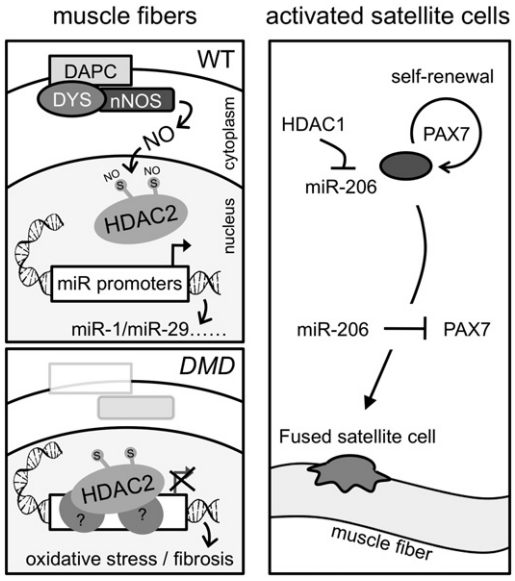

Figure 7. Model of the Pathway Connecting Dystrophin to Specific miRNA Expression

(Left panel) In WT muscle fibers the dystrophin/DAPC complex activates nNOS and S-nitrosylation of HDAC2. The modified HDAC2 is released from the chromatin and activation of a specific subset of miRNA occurs. In DMD this circuitry is deregulated due to impaired nNOS activity and decrease in HDAC2 nitrosylation, causing its retention to miRNA promoters. (Right panel) miR-206 follows an independent control from the other myomiRs: it is controlled by HDAC1 and expressed in activated satellite cells where it represses the Pax7 factor, thus allowing differentiation to proceed.

that could account for the observed morphofunctional benefits had been characterized. In this work, taking advantage of the exon-skipping strategy, we identified a specific group of miRNAs whose expression depends on dystrophin levels and whose deregulation explains several DMD pathogenetic traits. This class of miRNAs, poorly expressed in *mdx*, was upregulated in exon-skipping-treated animals and included muscle specific (miR-1 and miR-133) and more ubiquitous (miR-29 and miR-30) ones. The same miRNAs displayed a dystrophin-dependent upregulation also in human DMD myoblasts rescued for dystrophin synthesis through exon skipping.

The transcriptional activation of these miRNAs correlated with the acetylation state of H3K9 and modulation of HDAC2 binding to their promoters: in the absence of dystrophin, the low miRNA expression levels paralleled persistence of HDAC2 onto miRNA regulatory regions. On the contrary, when dystrophin synthesis was rescued, HDAC2 was released from miRNA promoters and transcription resumed. The use of mutated HDAC2 as well as treatment of *mdx* mice with NO donors indicated that the release of HDAC2 from the chromatin was due to its nitrosylation. Notably, we showed that as a consequence of dystrophin rescue, nNOS was stabilized and relocalized on the muscle membrane, and this directly affected the nitrosylation levels of HDAC2. Altogether, these data allowed us to conclude that dystrophin, nNOS, HDAC2 nitrosylation, and miRNAs are on the same regulatory pathway as indicated in the model of Figure 7.

At variance with the other myomiRs, mainly present in mature fibers, miR-206 was restricted to differentiating satellite cells; therefore, its higher levels in *mdx* and exon-skipping-treated animals were due to massive regeneration occurring in dystrophic muscles. The compartmentalized expression observed in vivo was confirmed in cultured satellite cells where miR-206 was shown to play the crucial function of repressing Pax7. This transcriptional factor, which is the mark of myogenic progenitor cells, has been described to regulate self-renewal of satellite cells and their entry into the program of skeletal muscle differentiation (Buckingham and Relaix, 2007).

Moreover, miR-206 differed from miR-1, also because it was shown to be under the HDAC1 control. This, together with the restricted expression in activated satellite cells before the onset of dystrophin synthesis, is consistent with miR-206 being independent from the Dys/nNOS pathway active in mature differentiated fibers. These data disclose a different function for the two members of the miR-1 family and provide a molecular mechanism for understanding how the switch between proliferation and differentiation of satellite cells can be obtained.

The differential regulation of miR-1 and miR-206 also allows us to suggest that the epigenetic control mediated by the late differentiation marker, dystrophin, is very likely important for increasing the robustness of the muscle differentiation program consolidating only the expression of those miRNAs involved in circuitries of terminal differentiation and tissue integrity.

Analysis of the targets of the modulated miRNAs underscored regulatory networks important for understanding the DMD physiopathology. One relevant discovery was the finding that miR-1 controls G6PD, a housekeeping enzyme encoded in mammals by an X-linked gene. G6PD has important functions in intermediary metabolism because it catalyzes the first step in the pentose phosphate pathway and provides reductive potential in the form of NADPH; in fact, through NADPH production, G6PD is required to maintain cytosolic GSH levels and to protect against free radical injury. Disruption of the G6PD gene in male mouse embryonic stem cells indicated that G6PD activity is dispensable for pentose synthesis but is essential to protect cells against even mild oxidative stress (Pandolfi et al., 1995). At variance with normal muscles, in degenerating fibers most of the NADPH produced is utilized in the O_2 to $O^{\circ-}_2$ conversion mediated by the Ca^{2+}-dependent activation of NOX (Gupte et al., 2006; Shkryl et al., 2009), suggesting that in dystrophic fibers G6PD may have an aberrant action in radical production. Indeed, in *mdx* fibers higher expression levels of NOX were detected (Shkryl et al., 2009), suggesting a major contribution of this enzyme to the well-documented oxidative stress occurring in these damaged muscles. Moreover, dystrophin-deficient cells were shown to be more susceptible to free radical induced injury when compared to normal cells, even though the two populations were equally susceptible to other forms of metabolic stress (Rando et al., 1998).

In line with these data, we demonstrated that while miR-1 was able to downregulate G6PD, decreasing the levels of GSH in normal muscles, in dystrophic ones the increase in G6PD did not correlate with GSH levels. In *mdx* muscles, where the NOX undergoes upregulation, most of the NO pool is utilized to convert superoxide species ($O^{\circ-}_2$) into peroxinitrite ($ONOO^{\circ-}$); indeed, we show that under these conditions HDAC2 is poorly nitrosylated, paralleling miR-1 repression and G6PD upregulation.

Exogenous modulation of this pathway, through G6PD or NOX inhibition, had consequent effects both in increasing HDAC2 nitrosylation and miR-1 upregulation. Finally, local overexpression of miR-1 in *mdx* muscles determined downregulation of G6PD and in turn increase of HDAC2 nitrosylation. Altogether, these data proved the existence of a feed-forward circuitry between G6PD and miR-1 through nitrosylation of HDAC2 (Figure 5E) and suggested that the regulatory network dependent on the Dys/nNOS pathway has physiological relevance in controlling also the oxidoreductase state of the injured muscle.

The relevant role of the identified dystrophin-dependent miRNAs in the DMD pathogenesis was also tested for mir-29. Its overexpression in the gastrocnemius of *mdx* animals indicated that not only the target mRNAs for collagen and elastin were specifically downregulated but also that the muscles recovered a phenotype with a strong reduction in fibrosis.

It has been shown that a specific domain of dystrophin is responsible for nNOS interaction (Wells et al., 2003; Lai et al., 2009). Notably, this domain is absent in several Beker mutants that produce a shorter but functional dystrophin; therefore, it is likely that the dystrophin-nNOS pathway could only play a consolidating function on muscle structure and that its malfunctioning would be nonetheless compatible with life.

Altogether these findings show a link between the dystrophin/nNOS pathway and important molecular circuitries, including specific miRNAs and their targets, which play an important role in muscle differentiation, homeostasis, and integrity. Moreover, the identified epigenetic signature might provide a useful tool for designing and monitoring the outcome of future clinical studies as well as for identifying specific genes, correlated with the DMD physiopathology, that might represent the basis for new therapeutic interventions.

EXPERIMENTAL PROCEDURES

Animal Treatments and Constructs

Six-week-old *mdx* mice were tail vein injected with 0.5–1 × 10^{12} genome copies of the AAV-U1#23 (AAV#23) or virus as described in Denti et al. (2006) and sacrificed after 4 weeks. Electroporation was performed on 6-week-old *mdx* as described in Donà et al. (2003). Plasmids carrying miR-29a/b cluster (p-miR-29a), miR-1-2 (p-miR-1), and miR-206 (p-miR-206) expression cassettes under the control of the U1snRNA promoter were utilized (Fazi et al., 2005). WT and mutant FLAG-HDAC2 plasmids were provided by Dr. A. Riccio and described in Nott et al. (2008). NTG treatments were performed on 6- to 18-week-old *mdx* mice by local injections of 0.3 mg/kg of NTG or physiological solution in tibialis or gastrocnemius muscles and sacrificed after 4 hr. Apocynin and 6-aminonicotinamide were administered to *mdx* mice by osmotic pumps (ALZET) as in Walker et al. (1999) and Gupte et al. (2006).

Cell Culture

Muscle satellite cells were cultured and differentiated as described in Rando and Blau (1994). The Duchenne primary myoblasts carrying exons 48–50 deletion were obtained from Telethon Biobank (Carlo Besta Institute, Milan) and infected with a lentiviral construct containing antisense sequences against the splice junctions of exon 51 (LV#51, Incitti et al., 2010). LNA miRNA Knockdown (Exiqon) treatment was performed according to Taulli et al. (2009).

Protein and miRNA In Situ Analyses

Western blot on total extracts, H&E staining, and in situ analyses on 7 μm thick gastrocnemius cryosections were performed as described in Denti et al. (2006). In situ hybridizations were performed with NCL-DYS2 (Novocastra) and nNOS (Santa Cruz). Immunoprecipitations on protein extracts were performed with antibody against S-nitroso-Cys (Sigma) according to manufacturer's specifications and revealed by western blot using an antibody against HDAC2 (Upstate). Masson's trichrome staining (Sigma) was performed according to manufacturer's specifications. miRNA in situ hybridization was performed in formaldehyde and EDC-fixed gastrocnemius cryosections according to Pena et al. (2009).

Chromatin Immunoprecipitation Assays

ChIP analysis was performed according to Ballarino et al., (2005) with the following antibodies: HDAC2 and RNA Pol II (Santa Cruz), HDAC1, HDAC4, acetylated H3-Lys9 (Upstate), and Flag (Sigma). The starting material was 1–3 mm^3 for tissue samples or 1–10 × 10^5 cultured cells. ChIP assays on DMD cells were performed using the EZ Magna ChIP Assay Kit (Millipore) following the manufacturer's specifications.

RNA procedures, enzymatic assays, and statistical analyses are available as Supplemental Information.

SUPPLEMENTAL INFORMATION

Supplemental Information includes five figures, one table, Supplemental Experimental Procedures, and Supplemental References and can be found with this article online at doi:10.1016/j.cmet.2010.07.008.

ACKNOWLEDGMENTS

We thank Prof. A. Riccio, Dr. M. Mora, Prof. P. Paggi, and Dr. L. Lombardi for providing material; Dr. De Angelis for helpful discussion; and Marcella Marchioni for technical support. D.C. is a recipient of a Microsoft research PhD fellowship. This work was partially supported by grants from Telethon (GGP07049 to I.B. and GGP06119 to A.M.); Parent Project Italia, EU project SIROCCO (LSHG-CT-2006-037900); ESF project "NuRNASu," IIT "SEED," PRIN, and BEMM; Fondazione Roma, EU project-Myoage, AFM (to A.M.); and AFM and EU projects Clinigene and DiMi (to A.A.).

Received: October 21, 2009
Revised: March 23, 2010
Accepted: June 30, 2010
Published online: August 19, 2010

REFERENCES

Aartsma-Rus, A., Fokkema, I., Verschuuren, J., Ginjaar, I., van Deutekom, J., van Ommen, G.J., and den Dunnen, J.T. (2009). Theoretic applicability of antisense-mediated exon skipping for Duchenne muscular dystrophy mutations. Hum. Mutat. *30*, 293–299.

Ballarino, M., Morlando, M., Pagano, F., Fatica, A., and Bozzoni, I. (2005). The co-transcriptional assembly of snoRNPs controls the biosynthesis of H/ACA snoRNAs in *S. cerevisiae*. Mol. Cell. Biol. *25*, 5396–5403.

Brenman, J.E., Chao, D.S., Xia, H., Aldape, K., and Bredt, D.S. (1995). Nitric oxide synthase complexed with dystrophin and absent from skeletal muscle sarcolemma in Duchenne muscular dystrophy. Cell *82*, 743–752.

Brunelli, S., Sciorati, C., D'Antona, G., Innocenzi, A., Covarello, D., Galvez, B.G., Perrotta, C., Monopoli, A., Sanvito, F., Bottinelli, R., et al. (2007). Nitric oxide release combined with nonsteroidal antiinflammatory activity prevents muscular dystrophy pathology and enhances stem cell therapy. Proc. Natl. Acad. Sci. USA *104*, 264–269.

Buckingham, M., and Relaix, F. (2007). The role of Pax genes in the development of tissues and organs: Pax3 and Pax7 regulate muscle progenitor cell functions. Annu. Rev. Cell Dev. Biol. *23*, 645–673.

Chen, J.F., Mandel, E.M., Thomson, J.M., Wu, Q., Callis, T.E., Hammond, S.M., Conlon, F.L., and Wang, D.Z. (2006). The role of microRNA-1 and microRNA-133 in skeletal muscle proliferation and differentiation. Nat. Genet. *38*, 228–233.

Colussi, C., Mozzetta, C., Gurtner, A., Illi, B., Rosati, J., Straino, S., Ragone, G., Pescatori, M., Zaccagnini, G., Antonini, A., et al. (2008). HDAC2 blockade by nitric oxide and histone deacetylase inhibitors reveals a common target in

Duchenne muscular dystrophy treatment. Proc. Natl. Acad. Sci. USA *105*, 19183–19187.

Colussi, C., Gurtner, A., Rosati, J., Illi, B., Ragone, G., Piaggio, G., Moggio, M., Lamperti, C., D'Angelo, G., Clementi, E., et al. (2009). Nitric oxide deficiency determines global chromatin changes in Duchenne muscular dystrophy. FASEB J. *23*, 2131–2141.

De Angelis, F.G., Sthandier, O., Berarducci, B., Toso, S., Galluzzi, G., Ricci, E., Cossu, G., and Bozzoni, I. (2002). Chimeric snRNA molecules carrying antisense sequences against the splice junctions of exon 51 of the dystrophin pre-mRNA induce exon skipping and restoration of a corrected phenotype in D48-50 DMD cells. Proc. Natl. Acad. Sci. USA *99*, 9456–9461.

Denti, M.A., Rosa, A., D'Antona, G., Sthandier, O., De Angelis, F.G., Nicoletti, C., Allocca, M., Pansarasa, O., Parente, V., Musarò, A., et al. (2006). Body-wide gene therapy of Duchenne Muscular Dystrophy in the mdx mouse model. Proc. Natl. Acad. Sci. USA *103*, 3758–3763.

Denti, M.A., Incitti, T., Sthandier, O., Nicoletti, C., De Angelis, F.G., Rizzuto, E., Auricchio, A., Musarò, A., and Bozzoni, I. (2008). Long-term benefit of adeno-associated virus/antisense-mediated exon skipping in dystrophic mice. Hum. Gene Ther. *19*, 601–608.

Donà, M., Sandri, M., Rossini, K., Dell'Aica, I., Podhorska-Okolow, M., and Carraro, U. (2003). Functional in vivo gene transfer into the myofibers of adult skeletal muscle. Biochem. Biophys. Res. Commun. *312*, 1132–1138.

Eisenberg, I., Eran, A., Nishino, I., Moggio, M., Lamperti, C., Amato, A.A., Lidov, H.G., Kang, P.B., North, K.N., Mitrani-Rosenbaum, S., et al. (2007). Distinctive patterns of microRNA expression in primary muscular disorders. Proc. Natl. Acad. Sci. USA *104*, 17016–17021.

Ervasti, J.M., and Sonnemann, K.J. (2008). Biology of the striated muscle dystrophin-glycoprotein complex. Int. Rev. Cytol. *265*, 191–225.

Fazi, F., Rosa, A., Fatica, A., Gelmetti, V., De Marchis, M.L., Nervi, C., and Bozzoni, I. (2005). A mini-circuitry comprising microRNA-223 and transcription factors NFI-A and C/EBPα regulates human granulopoiesis. Cell *123*, 819–831.

Ghahramani Seno, M.M., Graham, I.R., Athanasopoulos, T., Trollet, C., Pohlschmidt, M., Crompton, M.R., and Dickson, G. (2008). RNAi-mediated knockdown of dystrophin expression in adult mice does not lead to overt muscular dystrophy pathology. Hum. Mol. Genet. *17*, 2622–2632.

Greco, S., De Simone, M., Colussi, C., Zaccagnini, G., Fasanaro, P., Pescatori, M., Cardani, R., Perbellini, R., Isaia, E., Sale, P., et al. (2009). Common micro-RNA signature in skeletal muscle damage and regeneration induced by Duchenne muscular dystrophy and acute ischemia. FASEB J. *23*, 3335–3346.

Gupte, S.A., Levine, R.J., Gupte, R.S., Young, M.E., Lionetti, V., Labinskyy, V., Floyd, B.C., Ojaimi, C., Bellomo, M., Wolin, M.S., et al. (2006). Glucose-6-phosphate dehydrogenase-derived NADPH fuels superoxide production in the failing heart. J. Mol. Cell. Cardiol. *41*, 340–349.

Haslett, J.N., Sanoudou, D., Kho, A.T., Bennett, R.R., Greenberg, S.A., Kohane, I.S., Beggs, A.H., and Kunkel, L.M. (2002). Gene expression comparison of biopsies from Duchenne muscular dystrophy (DMD) and normal skeletal muscle. Proc. Natl. Acad. Sci. USA *99*, 15000–15005.

Incitti, T., De Angelis, F.G., Cazzella, V., Sthandier, O., Pinnarò, C., Legnini, I., and Bozzoni, I. (2010). Exon skipping and Duchenne Muscular Dystrophy therapy: selection of the most active U1 snRNA-antisense able to induce dystrophin exon 51skipping. Mol. Ther. Published online June 15, 2010. 10.1038/mt.2010.123.

Lai, Y., Thomas, G.D., Yue, Y., Yang, H.T., Li, D., Long, C., Judge, L., Bostick, B., Chamberlain, J.S., Terjung, R.L., et al. (2009). Dystrophins carrying spectrin-like repeats 16 and 17 anchor nNOS to the sarcolemma and enhance exercise performance in a mouse model of muscular dystrophy. J. Clin. Invest. *119*, 624–635.

Lee, Y., Kim, M., Han, J., Yeom, K.H., Lee, S., Baek, S.H., and Kim, V.N. (2004). MicroRNA genes are transcribed by RNA polymerase II. EMBO J. *23*, 4051–4060.

Liu, N., Williams, A.H., Kim, Y., McAnally, J., Bezprozvannaya, S., Sutherland, L.B., Richardson, J.A., Bassel-Duby, R., and Olson, E.N. (2007). An intragenic MEF2-dependent enhancer directs muscle-specific expression of microRNAs 1 and 133. Proc. Natl. Acad. Sci. USA *104*, 20844–20849.

Matsumura, K., Tomé, F.M., Collin, H., Leturcq, F., Jeanpierre, M., Kaplan, J.C., Fardeau, M., and Campbell, K.P. (1994). Expression of dystrophin-associated proteins in dystrophin-positive muscle fibers (revertants) in Duchenne muscular dystrophy. Neuromuscul. Disord. *4*, 115–120.

Minetti, G.C., Colussi, C., Adami, R., Serra, C., Mozzetta, C., Parente, V., Fortuni, S., Straino, S., Sampaolesi, M., Di Padova, M., et al. (2006). Functional and morphological recovery of dystrophic muscles in mice treated with deacetylase inhibitors. Nat. Med. *12*, 1147–1150.

Naguibneva, I., Ameyar-Zazoua, M., Polesskaya, A., Ait-Si-Ali, S., Groisman, R., Souidi, M., Cuvellier, S., and Harel-Bellan, A. (2006). The microRNA miR-181 targets the homeobox protein Hox-A11 during mammalian myoblast differentiation. Nat. Cell Biol. *8*, 278–284.

Nott, A., Watson, P.M., Robinson, J.D., Crepaldi, L., and Riccio, A. (2008). S-nitrosylation of histone deacetylase 2 induces chromatin remodelling in neurons. Nature *455*, 411–415.

Pandolfi, P.P., Sonati, F., Rivi, R., Mason, P., Grosveld, F., and Luzzatto, L. (1995). Targeted disruption of the housekeeping gene encoding glucose 6-phosphate dehydrogenase (G6PD): G6PD is dispensable for pentose synthesis but essential for defense against oxidative stress. EMBO J. *14*, 5209–5215.

Pena, J.T., Sohn-Lee, C., Rouhanifard, S.H., Ludwig, J., Hafner, M., Mihailovic, A., Lim, C., Holoch, D., Berninger, P., Zavolan, M., et al. (2009). miRNA in situ hybridization in formaldehyde and EDC-fixed tissues. Nat. Methods *6*, 139–141.

Rando, T.A., and Blau, H.M. (1994). Primary mouse myoblast purification, characterization, and transplantation for cell-mediated gene therapy. J. Cell Biol. *125*, 1275–1287.

Rando, T.A., Disatnik, M.H., Yu, Y., and Franco, A. (1998). Muscle cells from mdx mice have an increased susceptibility to oxidative stress. Neuromuscul. Disord. *8*, 14–21.

Rao, P.K., Kumar, R.M., Farkhondeh, M., Baskerville, S., and Lodish, H.F. (2006). Myogenic factors that regulate expression of muscle-specific microRNAs. Proc. Natl. Acad. Sci. USA *103*, 8721–8726.

Relaix, F., Montarras, D., Zaffran, S., Gayraud-Morel, B., Rocancourt, D., Tajbakhsh, S., Mansouri, A., Cumano, A., and Buckingham, M. (2006). Pax3 and Pax7 have distinct and overlapping functions in adult muscle progenitor cells. J. Cell Biol. *172*, 91–102.

Shkryl, V.M., Martins, A.S., Ullrich, N.D., Nowycky, M.C., Niggli, E., and Shirokova, N. (2009). Reciprocal amplification of ROS and Ca(2+) signals in stressed mdx dystrophic skeletal muscle fibers. Pflugers Arch. *458*, 915–928.

Taulli, R., Bersani, F., Foglizzo, V., Linari, A., Vigna, E., Ladanyi, M., Tuschl, T., and Ponzetto, C. (2009). The muscle-specific microRNA miR-206 blocks human rhabdomyosarcoma growth in xenotransplanted mice by promoting myogenic differentiation. J. Clin. Invest. *119*, 2119–2123.

Tseng, B.S., Zhao, P., Pattison, J.S., Gordon, S.E., Granchelli, J.A., Madsen, R.W., Folk, L.C., Hoffman, E.P., and Booth, F.W. (2002). Regenerated mdx mouse skeletal muscle shows differential mRNA expression. J. Appl. Physiol. *93*, 537–545.

van Rooij, E., Sutherland, L.B., Thatcher, J.E., DiMaio, J.M., Naseem, R.H., Marshall, W.S., Hill, J.A., and Olson, E.N. (2008a). Dysregulation of microRNAs after myocardial infarction reveals a role of miR-29 in cardiac fibrosis. Proc. Natl. Acad. Sci. USA *105*, 13027–13032.

van Rooij, E., Liu, N., and Olson, E.N. (2008b). MicroRNAs flex their muscles. Trends Genet. *24*, 159–166.

Walker, D.L., Reid, J.M., Svingen, P.A., Rios, R., Covey, J.M., Alley, M.C., Hollingshead, M.G., Budihardjo, I.I., Eckdahl, S., Boerner, S.A., et al. (1999). Murine pharmacokinetics of 6-aminonicotinamide (NSC 21206), a novel biochemical modulating agent. Biochem. Pharmacol. *58*, 1057–1066.

Wang, H., Garzon, R., Sun, H., Ladner, K.J., Singh, R., Dahlman, J., Cheng, A., Hall, B.M., Qualman, S.J., Chandler, D.S., et al. (2008). NF-kappa B-YY1-miR-29

regulatory circuitry in skeletal myogenesis and rhabdomyosarcoma. Cancer Cell *14*, 369–381.

Wehling, M., Spencer, M.J., and Tidball, J.G. (2001). A nitric oxide synthase transgene ameliorates muscular dystrophy in mdx mice. J. Cell Biol. *155*, 123–131.

Wells, K.E., Torelli, S., Lu, Q., Brown, S.C., Partridge, T., Muntoni, F., and Wells, D.J. (2003). Relocalization of neuronal nitric oxide synthase (nNOS) as a marker for complete restoration of the dystrophin associated protein complex in skeletal muscle. Neuromuscul. Disord. *13*, 21–31.

Yuasa, K., Hagiwara, Y., Ando, M., Nakamura, A., Takeda, S., and Hijikata, T. (2008). MicroRNA-206 is highly expressed in newly formed muscle fibers: implications regarding potential for muscle regeneration and maturation in muscular dystrophy. Cell Struct. Funct. *33*, 163–169.